Analytical Methods

Accepted Manuscript

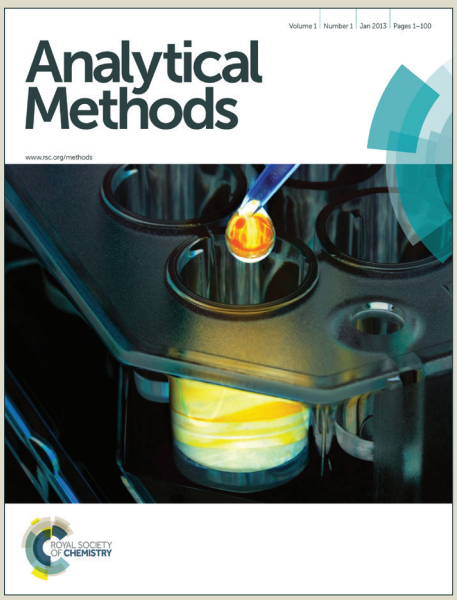

ROYAL SOCIETY OF CHEMISTRY

www.rsc.org/methods

Graphic Abstract:

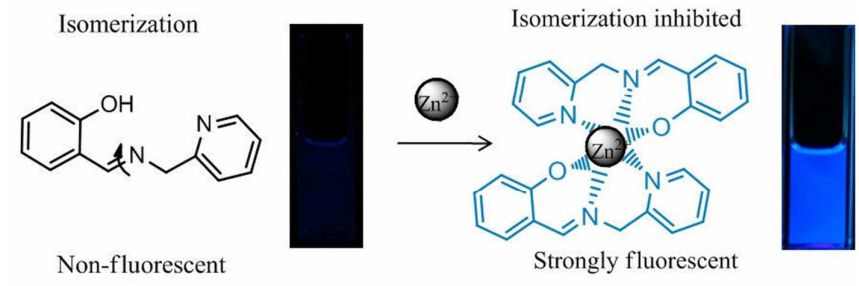

Proposed binding mechanism between receptor PPI and Zn(II). The method allows a simple and effective way for visual Zn(II) detection in environment.

Cite this: DOI: 10.1039/c0xx00000x

www.rsc.org/xxxxxx

ARTICLE TYPE

Highly Efficient Turn-on Fluorescence Detection of Zinc (II) Based on Multi-ligand Metal Chelation

Jian Sun,[§,a,b] Tao Yu,[§,c] Huan Yu,[a] Mingtai Sun,[a] Huihui Li,[a,b] Zhongping Zhang,[a,b] Hui Jiang,[c,*] and Suhua Wang[a,b,*]

Received (in XXX, XXX) Xth XXXXXXXXX 20XX, Accepted Xth XXXXXXXXX 20XX

DOI: 10.1039/b000000x

We report that the simple Schiff base molecule, 2-(((pyridin-2-ylmethyl)imino)methyl)phenol, can efficiently chelate zinc (II) to produce highly fluorescent complex, ML_2, which could be useful in the development of turn-on fluorescence detection of zinc (II). The compound initially shows very weak fluorescence, however, the coordination with zinc ion inhibits the C=N bond isomerization and subsequently enhances the fluorescence efficiency. Based on the turn-on fluorescence, the limit of detection for zinc (II) was measured to be 62 nM, which is lower than the allowable level of zinc (~ 70 μM) in drinking water set by U.S. Environmental Protection Agency. We tried to make fluorescence test strips by immobilizing the compound in silica gel plates and demonstrated the application for visualization of zinc screening in water and aerosol samples. The visual limit of detection was estimated as low as 9 μM.

1. Introduction

As the second most abundant transition metal ion in the human body and other mammals, zinc ion (Zn(II)) plays a significant role in various physiological and pathological processes, such as brain function,[1] signal transduction, gene transcription,[2] apoptosis regulation[3] and DNA binding or recognition.[4] It exists in various biological systems including brain, intestine, pancreas, retina, prostate, olfactory bulb, and spermatic sac.[5,6] Bound or mobile Zn(II) is believed to be an essential factor in many metalloenzymes and catalytic systems. The intracellular concentration of Zn(II) is tightly regulated and varies from picomolar to millimolar. Failure to keep Zn(II) homeostasis has been implicated in a series of pathological processes including Alzheimers disease,[7] cancer, epilepsy or ischemic stroke, and the imbalance of zinc could induce diarrhea, growth retardation and a lower immunity against infection.[8] Although Zn(II) is presumed to be less toxic, however, in the environment, an overweight of zinc is considered as a pollution that has been linked to the growth of detrimental soil bacteria and may induce the death of plants.[9] Therefore, it is of great importance to develop improved methods for quantifying and visualizing mobile Zn(II) in biological system and environment.

Due to the spectroscopically silence of Zn(II), the instant and real-time stoichiometrically detection of zinc ion still remains a great challenge. Current analytical techniques such as flame atomic absorption spectrometry (FAAS),[10,11] surface enhanced Raman scattering (SERS),[12] colorimetry[13] and ion selective electrode (ISE)[14] have been applied for analyses and detection of Zn(II). Beside these methods, fluorometry has been developed as a widely used technique. Recently, numerous fluorescent probes based on anthracene,[15] dansyl,[16] quinoline,[17] BODIPY,[18] coumarin[19] and fluorescein[20,21] have been utilized for detection of Zn(II). These widely used sensors reported up to now are designed in a number of mechanisms such as photoinduced electron/energy transfer (PET),[22] chelation-enhanced fluorescence (CHEF),[23] metal-ligand charge transfer (MLCT),[23,24] intramolecular charge transfer (ICT),[25,26] C=N isomerization,[23] and excited-state intra/intermolecular proton transfer (ESIPT).[27] Despite their attractive features, these currently developed fluorescence probes are commonly involved in complicated synthetic methods, expensive chemicals or tedious purification process. Simply structured Schiff bases and their derivatives are good ligands for transition metal ions and thus have been used in the design of molecular probe for biologically relevant transition-metal ions such as Zn(II), Cd(II), etc.[28,29,30]

Some of zinc-selective probes usually require complicated syntheses involving extreme reaction conditions and expensive chemicals. In this paper, we report a sensitive and selective turn-on fluorescence method, using the simple Schiff base molecule 2-(((pyridin-2-ylmethyl)imino)methyl)phenol (PPI) as the probe, for zinc (II) detection. This probe shows lower excitation energy, longer emission wavelength, and higher fluorescence enhancement efficiency by zinc. The Schiff base can be readily prepared with high yield by a simple one step reaction. Upon binding with Zn(II), the weak fluorescent probe PPI was greatly enhanced and showed highly fluorescence turn-on efficiency in a dose response manner with a high quantum yield.

2. Experimental

2.1 Materials and Chemicals

2-aminomethylpyridine and salicylaldehyde were purchased from Sigma Aldrich. Other chemicals and organic solvents were obtained from Shanghai Sangon Biotechnology Co and used without further purification. NaCl, KCl, $CaCl_2$, $CuCl_2{\cdot}2H_2O$, $BaCl_2$, $FeCl_3{\cdot}6H_2O$, $MgCl_2{\cdot}6H_2O$, $NiCl_2{\cdot}6H_2O$, $FeCl_3{\cdot}6H_2O$, $CoCl_2{\cdot}6H_2O$, $ZnCl_2$, $CdCl_2{\cdot}2.5H_2O$, $Pb(NO_3)_2$, $MnSO_4{\cdot}1H_2O$, $Hg(NO_3)_2$ were used to prepare metal ion stock solutions. $CDCl_3$ were used to record ^{1}H-NMR spectra. The ultrapure water (18.2 MΩ·cm) used to prepare aqueous solutions was produced from a Millipore water purification system and all glassware were cleaned successively with ultrapure water, and then dried before use.

2.2 Apparatus

The UV-vis absorption spectra were recorded with a Shimadzu UV-2550 spectrometer at room temperature. FT-IR spectra were obtained on Thermo Scientific iS10 infrared spectrometer. Fluorescence measurements were performed on a Perkin-Elmer LS-55 luminescence spectrometer (Llantrisant, UK) equipped with a plotter unit and a quartz cell (1 cm × 1 cm). ^{1}H NMR spectra were recorded on a Brucker Advance 400 NMR spectrometer, and mass spectra were obtained on a Thermo Proteome X-LTQ MS mass spectrometer in ESI positive mode. Silica gel-60 (230-400 mesh) was used as the solid phases for column chromatography. Thin-layer chromatography (TLC) was performed by using Merck F254 silica gel-60 plates. Photographs were taken by a Canon 350D digital camera.

2.3 Synthesis of 2-(((pyridin-2-ylmethyl)imino)methyl)phenol (PPI)

The probe PPI was synthesized as the following procedure. 2-(aminomethyl)pyridine (0.46 mL, 4.4 mM) was dissolved in CH_2Cl_2 (6 mL) in a 10 mL flask, followed by addition of salicylaldehyde (0.42 mL, 4 mM). The resulting solution turned yellow fleetly, after the mixture was stirred at room temperature for 4 hours, the solvent was evaporated to yield yellow oil on a rotary evaporator. The residue oil was further purified by flash Al_2O_3 column chromatography eluted with petroleum ether/dichloromethane (6:1 v/v) to give the desired product PPI (0.76 g, 3.6 mM, 90%) as pale yellow oil. ^{1}H NMR (400 MHz, $CDCl_3$, ppm): δ 13.28 (1H, s), 8.57 (1H, dd, J = 4.8,0.7 Hz), 8.54 (1H, s), 7.69 (1H, td, *J* = 7.7,1.8 Hz), 7.37 (1H, d, *J* = 7.8 Hz) , 7.35-7.29 (2H, m) , 7.21 (1H, dd, *J* = 7.1,5.3 Hz) , 6.97 (1H, d, *J* = 8.1 Hz), 6.90 (1H, td, *J* = 7.5,1.0 Hz), 4.95 (2H, s). ESI-MS (m/z): calcd for $C_{13}H_{12}N_2O$ 212.09, found 213.12 $[M + H]^+$.

2.4 Fluorescence experiments

A stock solution of probe PPI (0.1 M) was prepared by dissolving the probe (0.212 g) in ethanol (10 mL), the stock solution was then diluted to appropriate concentration for further experiments. 2 μL of the PPI solution (1 mM) was added into 2 mL of ethanol, and the final concentration of probe was 1.0 μM. The Zn(II) and other metal ions dissolved in water were added into the probe solution under the same conditions followed by recording the fluorescence spectra. All fluorescence emission spectra were recorded in the wavelength range from 392 nm to 650 nm using a 372 nm as an excitation wavelength and a 500 nm/min scan rate. The slit widths for excitation and emission were both 10 nm.

2.5 Fluorescence quantum yield measurement

Fluorescence quantum yield is measured using quinine sulfate as standard by the following procedure: Quinine sulfate in 0.1 M H_2SO_4 (quantum yield 0.54 at 372 nm) was chosen as a standard for the fluorescence quantum yield measurement. The values are calculated using the standard reference sample that has a fixed and known fluorescence quantum yield value, according to the following equation:

$$\boldsymbol{QY_s = QY_q * [A_s/A_q] * [F_q/F_S] * [\eta_s/\eta_q]^2 \qquad F = 1 - 10^{-D}}$$

Where *A* is the integrated emission intensity, *F* is fraction of light absorbed which can be calculated by the equation, η is the refractive index of the solvent for the solution, *D* is the absorbance at the excitation wavelength. The subscript "*q*" and "*s*" refers to the reference quinine sulfate and the probe PPI, respectively.

3. Results and discussion

3.1 Characterization and properties of the probe PPI

The probe PPI was synthesized with a high yield (~ 90%) by condensation reaction between 2-aminomethylpyridine and salicylaldehyde under mild conditions (Scheme S1). A portion of pure yellow oil was purified from the crude product by preparative TLC. The structure of the probe was confirmed by ESI-MS, ^{1}H NMR and FT-IR results. The ESI-MS spectrum shows a major peak at *m/z* 213.12 $[M + H]^+$, which matches perfectly with the calculated molecular weight of $[PPI]^+$ (Fig. S1). The ^{1}H NMR spectrum was further conducted to confirm the purity and the structure of the probe (Fig. S2). FT-IR spectrum obtained using the KBr pellet method (Fig. S3) shows a vibration band at 1650 cm^{-1} which can be assigned to the stretch of imide (-C=N-) groups in the PPI molecule. The vibration band at 3050 cm^{-1} was due to the pyridine ring, and the band at 670 cm^{-1} was attributed to the vibration of carbon hydrogen bond (-C-H).

The probe PPI shows a weak fluorescence peak at 430 nm with a negligible fluorescence quantum yield when it was excited at 372 nm. The weak fluorescence of probe PPI may be due to the C=N isomerization and the excited-state intra/intermolecular proton transfer (ESIPT) involving the phenolic protons of the salicylic amide moiety. However, the fluorescence intensity of the probe was greatly enhanced upon the addition of Zn(II), accompanied by a 30 nm bathochromic shift (Fig. S4). This clearly demonstrates that the fluorescence of PPI can be turned on by zinc ion, which was then utilized to design a turn-on fluorescence probe for visual detection of zinc ion.

The photostability of the probe PPI was evaluated by flashing consecutive UV light through an ethanol solution (1.0 μM PPI) under a Xenon light source with a power of 20 kW. After 60 consecutive illuminations (2 minutes for each time, λ_{ex} = 372 nm), there was no apparent change in fluorescence intensity (Fig. S5), indicating that the probe has a good photostability and is resistant to photo-bleaching. The effect of pH value on the fluorescence intensity of PPI was also examined in phosphate buffer-ethanol (50%, v/v) solution. The fluorescence intensity of PPI solution in Fig. S6 is weaker than in Fig. S5, it may be caused by the lower solubility of PPI after the addition of phosphate buffer. The

fluorescence intensity is nearly stable in the pH range from 4 to 11 (Fig. S6), suggesting that probe PPI is pH insensitive and this property makes it proper to be applied to biological systems and practical application.

3.2 Fluorescence titration and sensitivity

To investigate the sensitivity of the turn-on fluorescence probe for zinc ion detection, the fluorescence titration of PPI towards Zn(II) was carefully examined. For comparison, two concentrations of the probe were used for the experiments and the results were presented in Fig. 1 (1 μM) and Fig. 2 (10 μM), respectively. As illustrated in Fig. 1 inset, the fluorescence intensity was greatly increased 18 times by one molar equivalent of zinc ion. Also the inset shows the linear relationship between the fluorescence intensity and the amount of Zn(II) added. A correlation coefficient of 0.998 was obtained which can be used for the quantification of Zn(II). The limit of detection (LOD) was found to be 62 nM based on the definition of three times the deviation of the blank signal. When higher concentration of the probe (10 μM) was used, the fluorescence enhancement also exhibits a linear response versus the amount of zinc ion with a correlation coefficient of 0.996, as shown in Fig. 2. The results indicate that the probe can be used for Zn(II) detection in a wide concentration range.

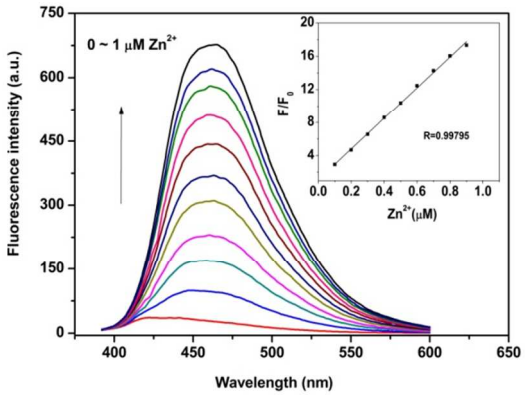

Fig. 1 Fluorescence enhancement of PPI in ethanol solution (1.0 μM) upon addition of increasing concentration of Zn(II) (0 - 1.0 μM). The inset plot is the calibration curve corresponding to the fluorescence intensity of the PPI versus the concentration of the Zn(II), the curve well fits a linear relationship with the concentration of Zn(II). F and F_0 are the fluorescence intensity of PPI in the presence and absence of Zn(II), respectively. The fluorescence spectra were recorded with excitation at 372 nm.

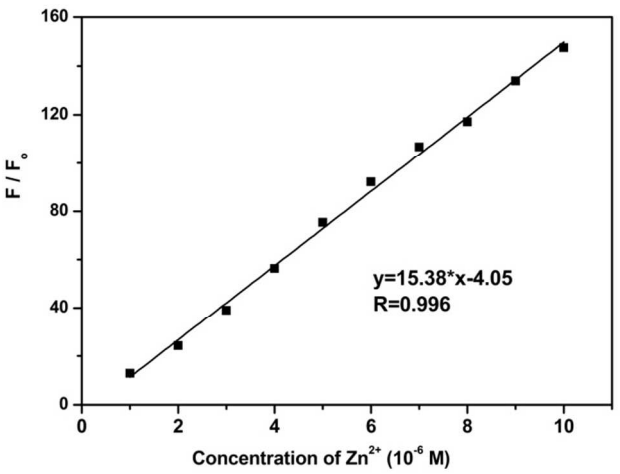

Fig. 2 Plot of fluorescence enhancement efficiency of the PPI in ethanol solution (10 μM) as a function of the Zn(II) in higher concentration range. F and F_0 were the fluorescence intensity of the PPI solution in the presence and absence of different concentrations of Zn(II), respectively. The fluorescence spectra were recorded with excitation at 372 nm.

3.3 The coordination between PPI and Zn(II)

In order to better understand the mechanism of the chemosensor of Zn(II) detection, stoichiometric reaction and the ESI-MS spectra were systematically carried out both in the absence and presence of Zn(II). The absorbance of the new peak at 372 nm was recorded as a function of molar ratio to validate the stoichiometry during the binding of Zn(II). Fig. 3 shows the Job's plot obtained by monitoring the absorbance at 372 nm. Clearly, the absorption reaches the maximum at the molar fraction of Zn(II) at 0.33, which suggests that the probe coordinates with zinc ion in a 2 : 1 stoichiometric manner. This is further confirmed by the ESI-MS spectra of the mixture, which displays a dominating peak at m/z = 487.02 $[M + H]^+$, consistent with the molecular weight of the complex $Zn(PPI)_2$ (486.12, Fig. S7).

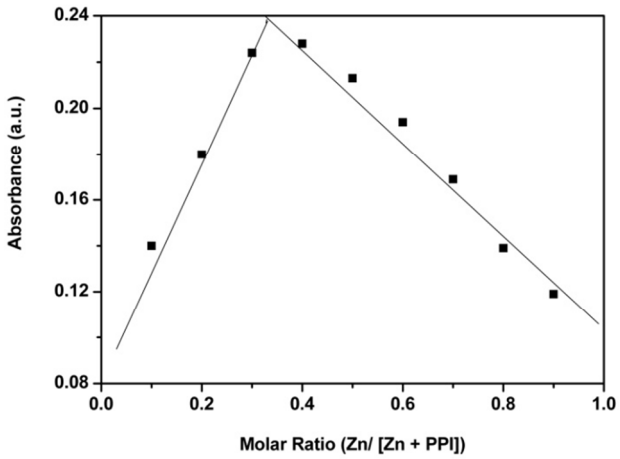

Fig. 3 Job's plot for the binding of PPI with Zn(II) in ethanol. Absorbance at 372 nm was plotted as a function of the molar ratio [Zn(II)] / ([PPI] + [Zn(II)]). The total of the concentration of PPI and Zn(II) is 120 μM.

The absorption spectral responses of PPI to zinc ion were investigated to understand the reaction mechanism, as shown in Fig. 4. Initially, the probe solution shows two absorption bands at 273 nm and 322 nm. Upon the addition of Zn(II), both the two

absorption bands decreased gradually, accompanied by appearance of a new absorption band at 372 nm. As the amount of zinc ion increased, three distinct isosbestic points at 250 nm, 290 nm and 337 nm formed, indicating the binding of the ligand with zinc ion. The new absorption band at 372 nm finally reached a plateau after excessive amount of zinc was added, as shown in Fig. 4 inset, which represents the simple titration curve based on the absorbance at 372 nm. These results suggest the formation of zinc complex $Zn(PPI)_2$. The absorbance at 372 nm was increased in the ratio with the added concentrations of Zn(II) (0 - 150 μM) with a good correlation equation of 0.999, which can also be used for quantitative zinc detection by absorption spectrometry. Moreover, the calibration curve was obtained in the low concentration range of Zn(II) added. Further addition of excess zinc ion leads to slight absorbance increase (data not shown). The association constant for $Zn(PPI)_2$ in ethanol was determinated to be 8.99×10^5 M^{-1} by a Hill plot.[31]

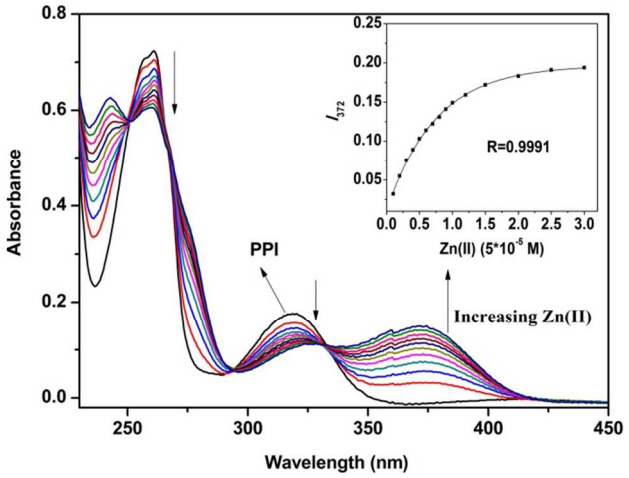

Fig. 4 UV-vis spectral responses of the probe PPI (50 μM) in ethanol to increasing amount of Zn(II) added. The three distinct isosbestic points at 250 nm, 290 nm and 337 nm indicate the formation of PPI-Zn. The inset plot is the calibration curve corresponding to the absorption intensity versus the concentrations of Zn(II) added.

The fluorescence quantum yields of the probe PPI and the complex $Zn(PPI)_2$ were measured, respectively. As shown in Fig. S8 and Table S1, the probe PPI has a low quantum yield of 1.29 % when excited at 372 nm. After reaction with zinc ion, the complex product $Zn(PPI)_2$ shows a high quantum yield of 25.9 %. The fluorescence enhancement due to chelation with zinc ion may be attributed to the inhibition of C=N isomerization and excited-state intra/intermolecular proton transfer (ESIPT) generated by the stable complexation.[23,32]

3.4 Reversibility of the fluorescence of the $Zn(PPI)_2$

The fluorescence of the complex $Zn(PPI)_2$ could be quenched if the chelation was broken by stronger ligand for zinc, such as ethylenediaminetetraacetic acid disodium salt (EDTA). Upon the addition of one equivalent of EDTA, the fluorescence of the complex $Zn(PPI)_2$ was greatly quenched, as shown in Fig. S9. When more Zn(II) was added into the solution, the fluorescence was proved to be turned on again. This result further confirms that the fluorescence enhancement of PPI by zinc ion could be attributed to the formation of complex $Zn(PPI)_2$ and then the chelation-enhanced fluorescence effect induced by Zn(II) chelation.

3.5 Selective response of PPI to Zn(II) and anti-interference study

In this work, the fluorescence responses of PPI upon the addition of various metal ions were carefully examined under the same conditions, as shown in Fig. 5. It can be seen that the addition of other metal ions including Na^+, K^+, Ba^{2+}, Cu^{2+}, Fe^{3+}, Mn^{2+}, Ni^{2+}, Cd^{2+}, Ca^{2+}, Mg^{2+}, Hg^{2+}, Co^{2+}, Pb^{2+} do not turn on the fluorescence of PPI. Only Zn(II) (1 μM) caused a significant fluorescence increasing. The results clearly show that PPI exhibited excellent selectivity towards Zn(II) over other cations in the assay conditions. The corresponding fluorescence spectra of PPI upon adding different metal ions (1 μM for PPI and other metal ions, 100 μM for Na^+ and K^+) were provided as Fig. S10. The high selective fluorescence enhancement by zinc could be due to the ESIPT of the PPI-Zn complex and the low electron attracting ability of zinc (II). Some metal ions could not complex with PPI such as Mn^{2+}, however, other metals such as Pb^{2+}, Cu^{2+}, and Cd^{2+} could also complex with PPI (as evidenced in Fig. S11), but their relative high electron attracting abilities greatly suppress the fluorescence enhancement.

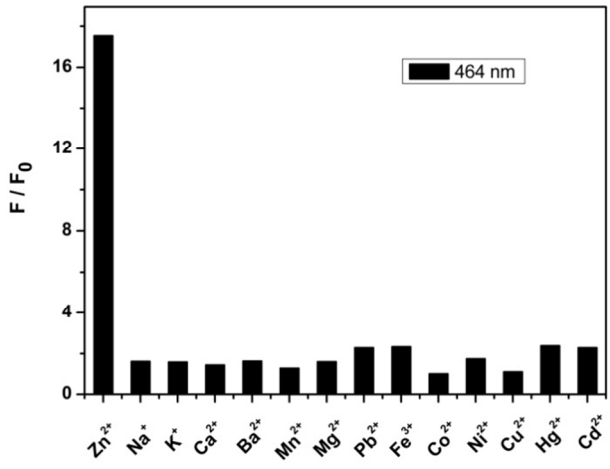

Fig. 5 Selectivity of the probe PPI in ethanol solution (1 μM) over other metal ions (100 μM for Na^+ and K^+, 1 μM for other metal ions, λ_{ex} = 372 nm). F_0 and F were the fluorescence intensity of PPI in the absence and presence of metal ions, respectively.

To evaluate the interference of other metal ions, the fluorescence turn-on experiments were performed in the presence of competing metal ions. The results clearly show that most of the cations have no interferences on the fluorescence turn-on by zinc ion (Fig. S12). It should be noted that Co^{2+}, Cu^{2+}, and Ni^{2+} cations show weak negative interference. This could be due to their competition reaction with PPI. Fortunately, the interference can be suppressed by a simple sample pretreatment with hyposulfite ion for the purpose of detecting Zn(II) (Fig. S13). These results show that the probe PPI exhibits good properties as a turn-on fluorescence probe for zinc ion detection.

3.6 Visual detection of Zn(II)

To make a portable fluorescence test strip for on-site visual screening of Zn(II), the probe PPI has been immobilized onto

silica gel plate. For visual detection of Zn(II), 2 μL of solution containing Zn(II) was carefully dropped on the plate sensor and subsequently was observed under a UV lamp illumination, as shown in Fig. 6. Clearly, the blue fluorescence dots were observed and their brightness is dependent on the amount of zinc ions added. The visual detection limit for Zn(II) was found to be 9 μM (0.6 ppm).

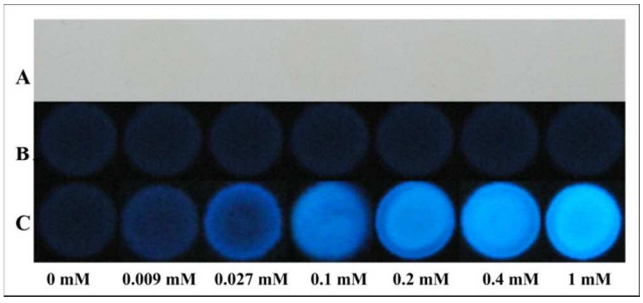

Fig. 6 The images of the chemosensors. (A) and (C) present the chemosensors after the addition of zinc solution with different concentrations (from left to right, 0 mM, 0.009 mM, 0.027 mM, 0.1 mM, 0.2 mM, 0.4 mM, 1 mM) under daylight and 365 nm UV lamp, respectively. (B) the chemosensor without the addition of zinc solution under a UV lamp illumination.

The visual detection method was also demonstrated for the semi-quantitative screening of Zn(II) in aerosol. The aerosol sample containing zinc chloride was prepared in a three-neck round bottom flask by the following procedure. The solution spray of 5 mM zinc chloride solution was injected into a nitrogen flow to form the aerosol in the flask. The nitrogen gas containing the aerosol was flowed over a fluorescence test strip for 5 min, which was covered with a piece of plastic paper hollowed-out with an element symbol of "Zn". A clear blue symbol of "Zn" was observed on the test strip under the illumination of a UV lamp when the piece of plastic paper was removed (Fig. 7). The result suggests that the method can be utilized for zinc (II) screening in aerosol. A further research for quantitative determination of zinc (II) in aerosol is in progress.

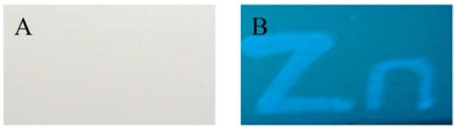

Fig. 7 Illustration of the fluorescence test strip for visual determination of zinc (II) in aerosol. Photos of the test strip exposed to zinc chloride aerosol, (A) under daylight and (B) under UV light.

3.7 Recovery test of Zn(II) in real water sample

The recovery test of zinc ion was conducted in tap water and local lake water, respectively, to examine if there is interference in real water samples. The real lake water was collected from a local Shushan lake and filtered through 0.45 μm Supor filters to remove any particulate suspension. We first examined the effect of water on the fluorescence and found no enhancing effect. The recovery studies were carried out on the samples spiked with 0.2, 1 and 2 μM zinc chloride. The fluorescence intensities of PPI were recorded before and after addition of zinc ion. Each concentration was done for three times under the same condition and the average was presented with standard deviation. Table 1 summarizes the results and it can be seen that there are differences between tap water and lake water sample. The recoveries in tap water samples are statistically close to those values spiked. But the recoveries in real lake water are lower than tap water, indicating that the organic contaminants and humic materials exhibit negative interferences for the detection of zinc ion. So the results are reasonable, showing that the probe for zinc detection is reliable and possesses the potential to be used in real samples.

Table 1. The detection of Zn(II) in Zn(II)-Spiked (1) Tap water and (2) Shushan Lake water by the probe

Spiked Zn(II) Concentration (μM)	Tap water		Lake water	
	Found (μM)	Recovery (%)	Found (μM)	Recovery (%)
0.2	0.196	98.3 ± 2.09	0.181	90.3 ± 4.24
1.0	1.037	103.7 ± 3.05	0.824	82.4 ± 3.87
2.0	1.930	96.5 ± 3.32	1.693	84.5 ± 6.58

4. Conclusions

A turn-on fluorescent probe containing a Schiff base as metal binding site for zinc ion has been synthesized through a condensation reaction. The chemical structure and spectral properties were carefully characterized. Selective binding with zinc ion greatly increased the fluorescence of the probe due to the formation of a rigid structure between the imine and zinc ion, which inhibits the C=N isomerization and excited-state intramolecular proton transfer. The chelation also causes a large chelation-enhanced fluorescence effect, leading to the fluorescence enhancement. Besides, the good selectivity towards Zn(II) was demonstrated in the presence of other metal ions. The method allows a simple and effective way for visual Zn(II) detection.

Acknowledgements

This work was supported by the National Basic Research Program of China (2011CB933700), the National Natural Science Foundation of China (Nos. 21205120, 21302187) and the Innovation Project of Chinese Academy of Sciences (KJCX2-YW-H29).

Notes and references

[a]*Institute of Intelligent Machines, Chinese Academy of Sciences, Hefei, Anhui, 230031, China. E-mail: shwang@iim.ac.cn.*
[b]*Department of Chemistry, University of Science & Technology of China, Hefei, Anhui, 230026, China. E-mail: shwang@iim.ac.cn*
[c]*Beijing Institute of Pharmaceutical Chemistry, State Key Laboratory of NBC Protection for Civilian, Beijing, 102205, China. E-mail: jiangtide@sina.cn.*
[§]These two authors contributed equally to this work.

† Electronic Supplementary Information (ESI) available: [details of any supplementary information available should be included here]. See DOI: 10.1039/b000000x/

1 E. Mocchegiani, C. Bertoni-Freddari, F. Marcellini, M. Malavolta, *Prog. Neurobiol.*, 2005, **75**, 367-390.
2 G. K. Andrews, *Biochem. Pharmacol.*, 2000, **59,** 95-104.
3 Y.-H. Kim, E. Kim, B. Gwag, S. Sohn, J.-Y. Koh, *Neuroscience.*, 1999, **89**, 175-182.
4 D. J. Segal, B. Dreier, R. R. Beerli, C. F. Barbas, Proc. *Natl. Acad. Sci. U S A.*, 1999, **96**, 2758-2763.
5 A. Takeda, *Biometals.*, 2001, **14**, 343-351.

6 C. J. Frederickson, L. J. Giblin III, B. Rengarajan, R. Masalha, C. J. Frederickson, Y. Zeng, E. V. Lopez, J.-Y. Koh, U. Chorin, L. Besser, *J. Neurosci. Methods.*, 2006, **154,** 19-29.

7 H. Kozlowski, M. Luczkowski, M. Remelli, D. Valensin, *Coor. Chem. Rev.*, 2012, **256**, 2129-2147.

8 A. H. Shankar, A. S. Prasad, *Am. J. Clin. Nutr.*, 1998, **68,** 447S-463S.

9 M. L. Guerinot, D. Eidet, *Curr. Opin. Plant. Biol.*, 1999,**2**, 244-249.

10 K. Fuwa, P. Pulido, R. McKay, B. L. Vallee, *Anal. Chem.*, 1964, **36**, 2407-2411.

11 R. L. Dutra, H. F. Maltez, E. Carasek, *Talanta.*, 2006, **69**, 488-493.

12 Y. Zhao, J. N. Newton, J. Liu, A. Wei, *Langmuir.*, 2009, 25 13833-13839.

13 Z. Xu, G.-H. Kim, S. J. Han, M. J. Jou, C. Lee, I. Shin, J. Yoon, *Tetrahedron.*, 2009, **65**, 2307-2312.

14 V. S. Vassilev, S. H. Hadjinikolova, S. V. Boycheva, *Sens. Actuators B.*, 2005, **106**, 401-406.

15 E. U. Akkaya, M. E. Huston, A. W. Czarnik, *J. Am. Chem. Soc.*, 1990, **112**, 3590-3593.

16 T. Koike, T. Watanabe, S. Aoki, E. Kimura, M. Shiro, *J. Am. Chem. Soc.*, 1996, **118**, 12696-12703.

17 Y. Zhang, X. Guo, W. Si, L. Jia, X. Qian, *Org. Lett.*, 2008, **10**, 473-476.

18 A. Ojida, T. Sakamoto, M.-a. Inoue, S.-h. Fujishima, G. Lippens, I. Hamachi, *J. Am. Chem. Soc.*, 2009, **131,** 6543-6548.

19 J.-S. Wu, W.-M. Liu, X.-Q. Zhuang, F. Wang, P.-F. Wang, S.-L. Tao, X.-H. Zhang, S.-K. Wu, S.-T. Lee, *Org. Lett.*, 2007, **9**, 33-36.

20 T. Hirano, K. Kikuchi, Y. Urano, T. Higuchi, T. Nagano, *J. Am. Chem. Soc.*, 2000, **122**, 12399-12400.

21 G. K. Walkup, S. C. Burdette, S. J. Lippard, R. Y. Tsien, *J. Am. Chem. Soc.*, 2000, **122**, 5644-5645.

22 T. Gunnlaugsson, A. P. Davis, J. E. O'Brien, M. Glynn, *Org. Lett.*, 2002, **4,** 2449-2452.

23 H. Y. Lin, P. Y. Cheng, C. F. Wan, A. T. Wu, *Analyst.*, 2012, **137,** 4415-4417.

24 M.-J. Kim, R. Konduri, H. Ye, F. M. MacDonnell, F. Puntoriero, S. Serroni, S. Campagna, T. Holder, G. Kinsel, K. Rajeshwar, *Inorg. Chem.*, 2002, **41**, 2471-2476.

25 L. Xue, Q. Liu, H. Jiang, *Org. Lett.*, 2009, **11,** 3454-3457.

26 L. Xue, C. Liu, H. Jiang, *Org. Lett.*, 2009, **11**, 1655-1658.

27 X. Zhang, L. Guo, F.-Y. Wu, Y.-B. Jiang, *Org. Lett.*, 2003, **5**, 2667-2670.

28 D. M. Epstein, S. Choudhary, M. R. Churchill, K. M. Keil, A. V. Eliseev, J. R. Morrow, *Inorg. Chem.*, 2001, **40**, 1591-1596.

29 S. Kim, J. Y. Noh, K. Y. Kim, J. H. Kim, H. K. Kang, S.-W. Nam, S. H. Kim, S. Park, C. Kim, J. Kim, *Inorg. Chem.*, 2012, **51**, 3597-3602.

30 L. Salmon, P. Thuéry, E. Rivière, M. Ephritikhine, *Inorg. Chem.*, 2006, **45**, 83-93.

31 S. Hisaindee, O. Zahid, M. A. Meetani, J. Graham. J. Fluoresc., .2012, **22**, 677–683.

32 J. Wu, W. Liu, J. Ge, H. Zhang, P. Wang, *Chem. Soc. Rev.*, 2011, **40**, 3483-3495.